Report

Cell Reports

Direct Neural Conversion from Human Fibroblasts Using Self-Regulating and Nonintegrating Viral Vectors

Graphical Abstract

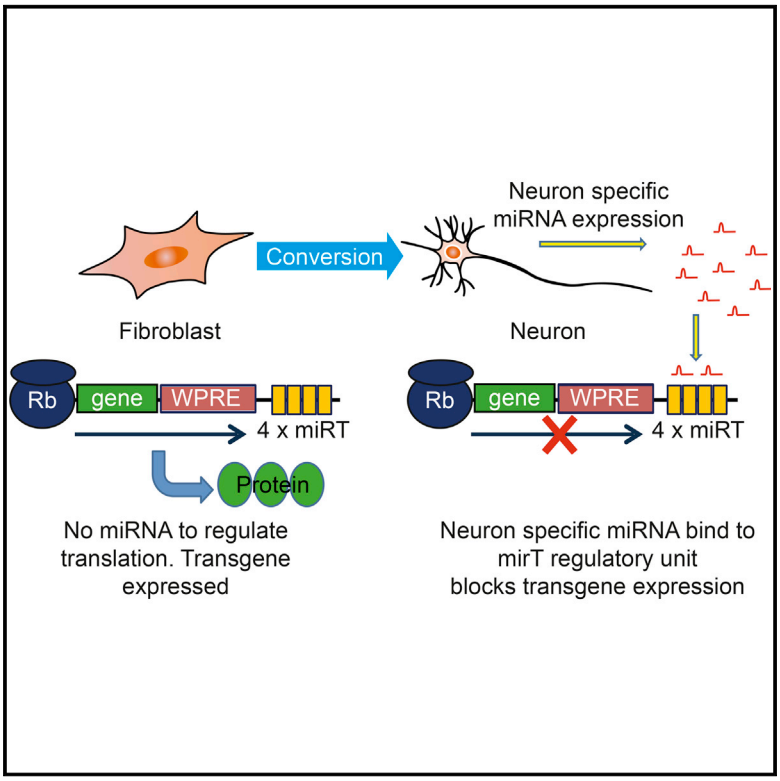

Highlights

Self-regulating neural conversion vectors are achieved by microRNA regulation

Cell-specific regulation of conversion factors improves functional maturation

The vector system results in remarkably high neural conversion

Nonintegrative, regulated vectors provide a clinically relevant conversion system

Authors

Shong Lau, Daniella Rylander Ottosson, Johan Jakobsson, Malin Parmar

Correspondence

malin.parmar@med.lu.se

In Brief

Lau et al. now use miRNA targeting to build a self-regulating neural conversion system. Combined with nonintegrating vectors, this system can efficiently drive conversion of human fibroblasts into functional induced neurons (iNs) suitable for clinical applications.

Lau et al., 2014, Cell Reports 9, 1673–1680
December 11, 2014 ©2014 The Authors
http://dx.doi.org/10.1016/j.celrep.2014.11.017

Cell Reports
Report

Direct Neural Conversion from Human Fibroblasts Using Self-Regulating and Nonintegrating Viral Vectors

Shong Lau,[1] Daniella Rylander Ottosson,[1] Johan Jakobsson,[1] and Malin Parmar[1,*]
[1]Department of Experimental Medical Science, Wallenberg Neuroscience Center and Lund Stem Cell Center, Lund University, BMC A11, 221 84 Lund, Sweden
*Correspondence: malin.parmar@med.lu.se
http://dx.doi.org/10.1016/j.celrep.2014.11.017

SUMMARY

Recent findings show that human fibroblasts can be directly programmed into functional neurons without passing via a proliferative stem cell intermediate. These findings open up the possibility of generating subtype-specific neurons of human origin for therapeutic use from fetal cell, from patients themselves, or from matched donors. In this study, we present an improved system for direct neural conversion of human fibroblasts. The neural reprogramming genes are regulated by the neuron-specific microRNA, miR-124, such that each cell turns off expression of the reprogramming genes once the cell has reached a stable neuronal fate. The regulated system can be combined with integrase-deficient vectors, providing a nonintegrative and self-regulated conversion system that rids problems associated with the integration of viral transgenes into the host genome. These modifications make the system suitable for clinical use and therefore represent a major step forward in the development of induced neurons for cell therapy.

INTRODUCTION

Functional, subtype-specific neurons can be obtained by direct conversion of human fibroblasts (Caiazzo et al., 2011; Liu et al., 2013; Pfisterer et al., 2011a; Son et al., 2011). The resulting cells are termed human induced neurons (hiNs). With only few exceptions, the growing number of studies reporting direct conversion of fibroblasts to neurons use doxycycline-regulated lentiviral vectors (Pfisterer et al., 2011a; Caiazzo et al., 2011; Liu et al., 2013; Vierbuchen et al., 2010; Dell'Anno et al., 2014; Wapinski et al., 2013). Although this technology is efficient for experimental studies, it is problematic from a clinical perspective. First, lentiviral vectors are integrating retroelements that have the capacity to affect gene expression levels of endogenous genes that can lead to transformation events (Nienhuis et al., 2006; Okita et al., 2008). Second, the doxycycline-regulated systems that have been used to "shut off" transgene gene expression after conversion are not optimal for clinical use because they contain elements of bacterial origin and require a continuous delivery of doxycycline to keep genes active (Gossen and Bujard, 1992). In this study, we describe an approach that circumvents these issues and allows for generation of functional iN cells using nonintegrating, self-regulating lentiviral vectors.

RESULTS

We, and others, have previously used miRNA-regulated vectors to control expression and efficiently visualize and isolate different cell populations (Åkerblom et al., 2013; Brown et al., 2007; Gentner and Naldini, 2012; Sachdeva et al., 2010). In this study, we used miR-124 to regulate neural conversion genes. MiR-124 is expressed exclusively in neurons, is known to promote neurogenesis in vitro and in vivo, and also has a potential role in regulating activities of postmitotic neurons (Åkerblom et al., 2012; Cheng et al., 2009; Krichevsky et al., 2006). To achieve self-regulation of our conversion vectors, we inserted four complementary binding sites of miR-124 (Figure 1A). Thus, in cells where miR-124 is not expressed (like the fibroblasts) the mRNA is not inhibited or degraded resulting in high-level expression of conversion factors. When a stable neuronal fate is reached during the conversion process, the hiN will turn on endogenous miR-124, which will then bind to the miR-target sequence in the vector-derived mRNA and efficiently inhibit the expression of the conversion factors. Thus, the system is self-regulating, alleviating the need for supply of drugs or chemicals for gene regulation. Additionally, the regulation is achieved on a cell-by-cell basis rather than on a population basis.

A prerequisite for the technique to work is that MiR-124 is expressed at high enough levels in the converted neurons. To establish this, we converted human fibroblast into hiNs by delivering lentiviral vectors coding for *Ascl1*, *Brn2*, and *Myt1L* (ABM). The resulting hiNs were sorted using a human specific neural cell adhesion molecule (hNCAM) at different time points, and miR-124 level was monitored using locked nucleic acid (LNA) quantitative RT-PCR (qPCR). For all time points analyzed, the hNCAM-positive population expressed miR-124, and the expression level increased upon maturation and then stabilized (Figure 1B).

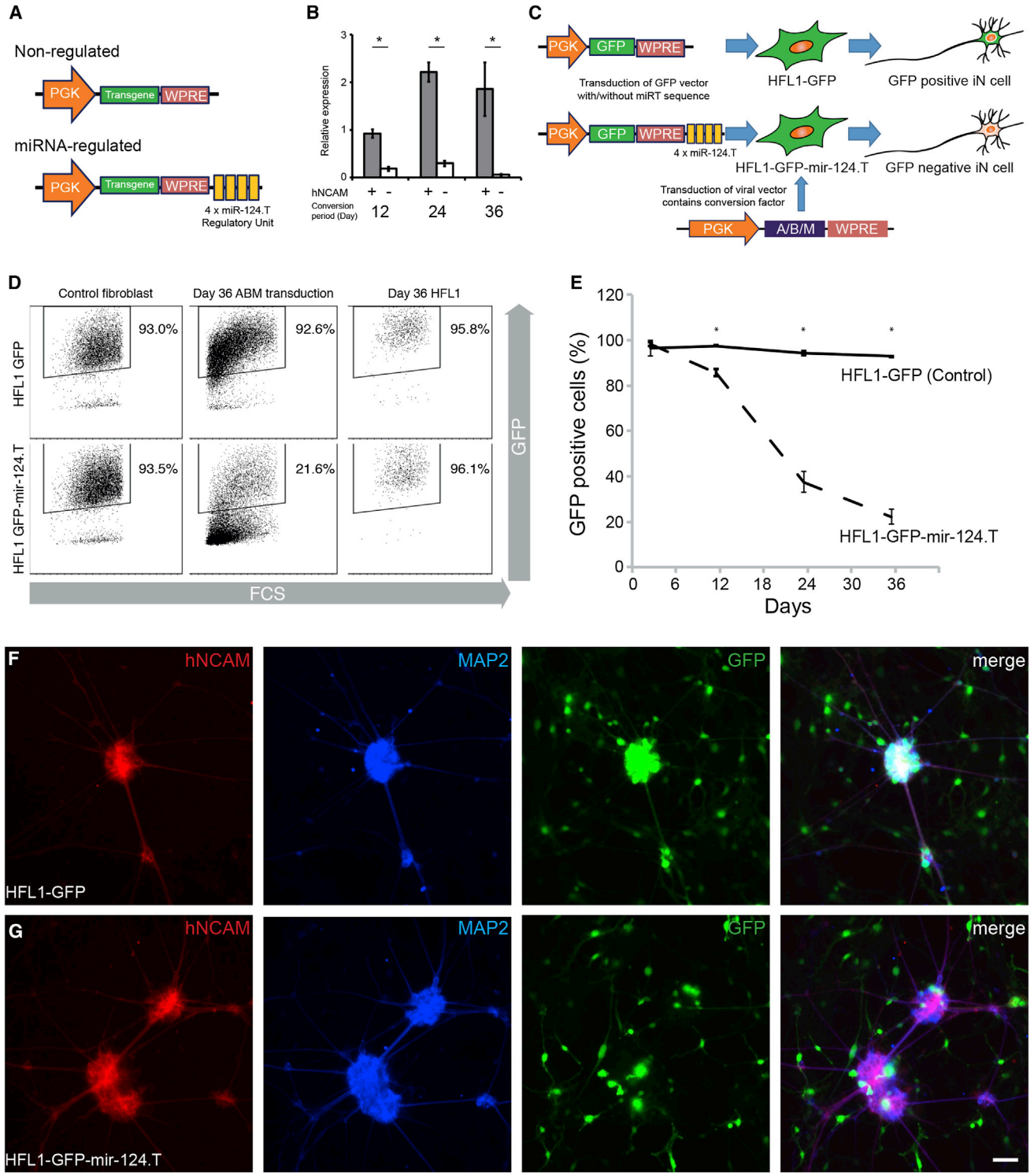

Figure 1. miR-124 Is a Neuron-Specific miRNA

(A) Vector maps of regulated and unregulated construct. In neurons that express miR-124, the target site (miRT) in the transcript is suppressed, resulting in no protein translation.

(B) LNA-qRT-PCR for sorted hNCAM-positive and hNCAM-negative hiN at various maturation stage (n = 3).

(C) Schematic representation of the vectors and experimental approach to generate miR-124.T reporter fibroblast cell line and subsequent conversion to GFP-positive and GFP-negative hiN.

(legend continued on next page)

We next investigated the potential of miR-124-regulated vectors to segregate transgene expression between human fibroblast and converted hiNs. We established stable GFP-expressing HFL1 cells with a lentiviral vector containing a GFP reporter gene followed by four copies of perfect matching miR-124-target sequences (HFL1-GFP-miR-124.T). Thus, GFP from this construct is regulated by miR-124, and consequently GFP can be used to monitor the activation of functional miR-124 during iN conversion. We also established a nonregulated GFP-only control cell line (HFL1-GFP). Upon conversion using ABM, the miR-124.T-regulated GFP is expected to be downregulated when the cells have reached a stable neuronal fate and start to express miR-124, whereas the iNs from control cells should remain GFP expressing (Figure 1C). In line with this, we found that GFP levels were downregulated in hiNs obtained from HFL1-GFP-miR-124.T upon neural conversion, whereas GFP-levels remained high throughout the conversion period in unregulated control HFL1-GFP cells (Figures 1D and 1E). Immunofluorescence staining confirmed that the hiN cells, detected using hNCAM and MAP2, were GFP negative in HFL1-GFP-miR124.T cells and GFP positive in HFL1-GFP control cells (Figures 1F and 1G). We observed no downregulation of GFP in the hNCAM-negative fraction of HFL1-GFP-miR-124.T or in HFL1-GFP control cells, confirming that downregulation of GFP only occurs in the converted hiNs (Figures S1A and S1B). Unconverted HFL1-GFP-miR-124.T and HFL1-GFP fibroblasts also expressed high-level GFP (Figures S1A and S1B). When fibroblasts were converted with *Ascl*1 alone (A), or in combination with *Brn2* (AB) or *Myt1L* (AM), no substantial downregulation of GFP were detected (Figure S1C). These data establish that hiNs converted using ABM start to express endogenous miR-124 that efficiently downregulate transgene expression upon conversion using miR-124.T-regulated vectors, validating the approach of using this vector system for self-regulating neural conversion.

Next, we assessed whether conversion factors placed under miR-124.T regulation could drive conversion of human fibroblasts to neurons. We transduced HFL1 cells with the miR-124.T-regulated conversion vectors (ABM-miR-124.T), nonregulated ABM vectors, and also cultured untransduced control cells in parallel (Figure S2A). Twelve days after initiation of conversion, we found an obvious morphology change in cells from both conversion groups (Figure S2B), and at day 24 we found similar numbers of hiN cells expressing the neuronal marker MAP2 (Figure S2C). No converted hiNs were detected in the control cells grown in parallel. Quantifications performed on days 12 and 24 posttransduction demonstrated comparable efficiency and purity when using ABM-miR-124.T compared to nonregulated vectors (Figures 2A, 2B, and S2D). Both the ABM-miR-124.T- and ABM-converted hiN cells expressed the neuronal markers NeuN (Figures 2C and 2D) and synaptophysin (SYP, Figures 2E and 2F) when analyzed 50 days posttransduction. qPCR analysis of the resulting hiN cells showed expression of *MAP2*, Synapsin (*SYN1*), and *SYP* (Figure 2G), confirming their neuronal identity, as well as expression of genes typically expressed by GABAergic (*GAD67*, *ISL1*, and *DARPP-32*) and glutamatergic (*VGLUT*, *TBR1*, and *TBR2*) neurons (Figure 2G), in a pattern that is similar to what we have previously observed for iN cells converted using standard vectors (Pereira et al., 2014). These data demonstrate that miR-124.T-regulated vectors stably convert human fibroblasts to induced neurons at the same efficiency and purity as nonregulated vectors, without significant effects on subtype specificity. It is worth noting that the conversion efficiency is remarkably high in these experiments compared to most other published studies (Ambasudhan et al., 2011; Caiazzo et al., 2011; Davila et al., 2013; Pang et al., 2011; Pfisterer et al., 2011a; Wang et al., 2014; Yoo et al., 2011), and on par with the highest conversion efficiencies that have been reported using doxycycline-regulated vectors (Ladewig et al., 2012; Liu et al., 2013; Pereira et al., 2014). One likely explanation for this is the use of phosphoglycerate kinase (PGK) promoter in these studies. The PGK promoter results in robust, ubiquitous, moderate level transgene expression, with very little tendency to transgene silencing/variation, which may be optimal for iN conversion.

An additional advantage of using microRNA regulation is that the regulation is achieved in a cell-autonomous manner. Thus, the reprogramming genes are turned off only in cells that have reached a stable neuronal fate and not on a population basis by withdrawal of doxycycline. This could minimize the presence of partially reprogrammed hybrid cells that can occur if reprogramming is incomplete in the cells (Okita et al., 2007; Polo et al., 2012; Takahashi and Yamanaka, 2006).

We next used patch-clamp electrophysiology to investigate the functional properties of the neurons obtained using the regulated and nonregulated conversion system. First, we confirmed that there were no obvious differences in the electrophysiological properties of hiN cells generated with the standard doxycycline-regulated vectors and hiNs obtained using the PGK promoter to drive transgene expression. (Figure S2E). We then investigated and compared the functional properties of ABM-miR-124.T and ABM-converted hiN cells in more detail. Cells in both groups showed functional electrophysiological properties with evoked repetitive or single action potentials after current injections (Figures 2H–2J, n = 20 for ABM and 11 for ABM-miR124.T). At 60 days postconversion, a higher proportion of ABM-mi-124.T-converted cells were able to evoke more action potentials (Figure 2K). Both cell types exhibited fast inactivated inward and outward current characteristic of sodium and delayed-rectifier potassium currents (Figures 2L and 2M). However, the regulated group showed greater inward sodium currents (Figure 2N) compared to ABM nonregulated cells. Occasional postsynaptic events, indicating formation of synaptic networks, could be seen in both groups: four of 17 for ABM and four of 19 for ABM-miR-124.T (Figure 2O). Both action potentials and inward currents could be blocked with TTX (Figures S2F–S2I). Long-term measurement at 90 days postconversion

(D) Flow cytometry analysis of GFP positivity in hNCAM-positive cells of day 36 hiN culture.
(E) Quantification of GFP-positive cell in hNCAM-positive cells of hiN culture at various maturation stage (n = 3).
(F and G) hNCAM- and MAP2-positive cells derived from GFP labeled HFL1 on day 36 of hiN conversion.
Scale bar, 100 μm. See also Figure S1.

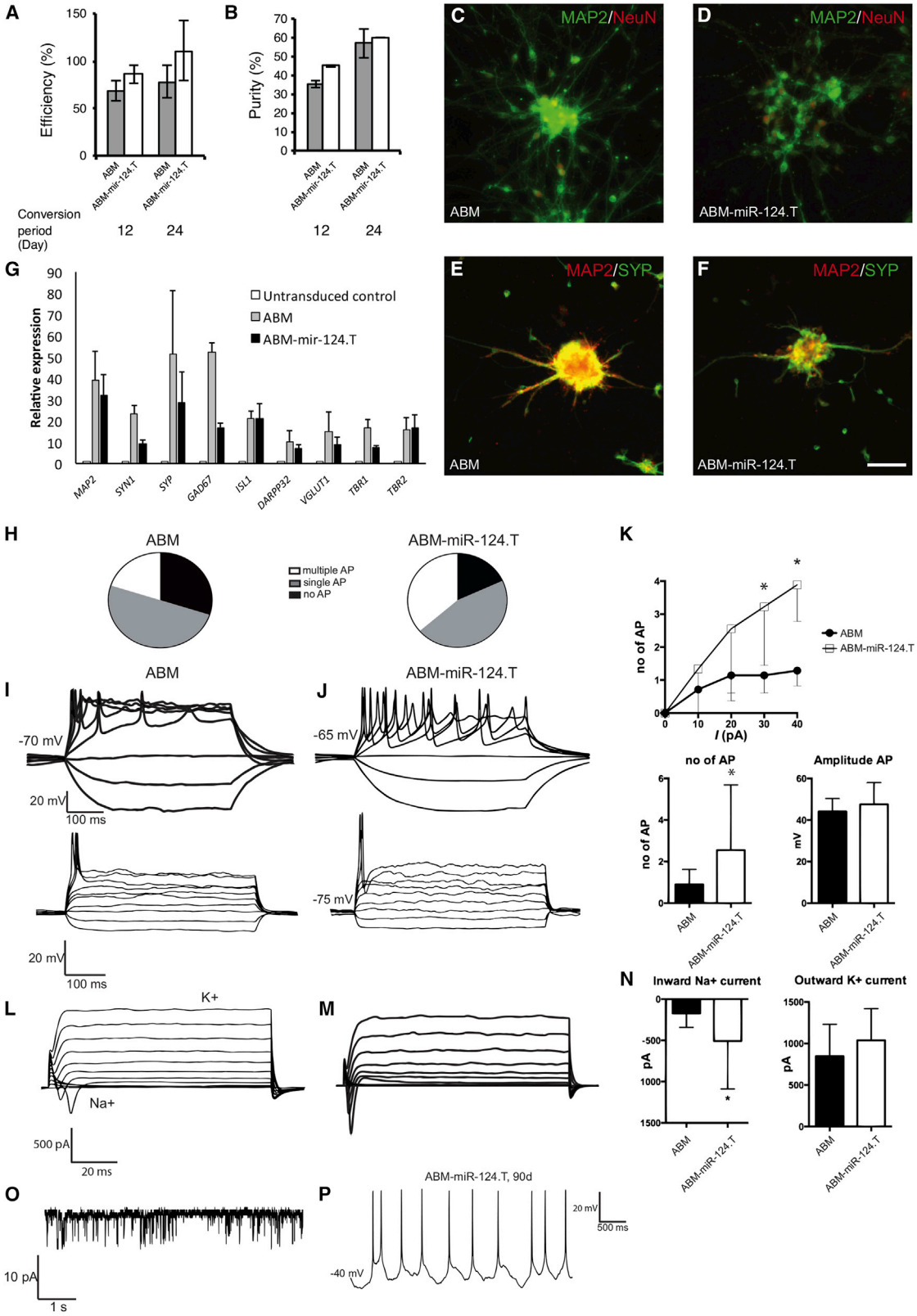

(legend on next page)

still revealed healthy and morphologically mature neurons in both groups, and, interestingly, at this time, regulated iNs had started to show spontaneous firing (n = 5/11 for ABM-miR-124.T, Figure 2P), whereas the nonregulated hiN cells did not (n = 0/6). Taken together, these data suggest that hiN cells where the neural conversion genes are downregulated after stable conversion achieved more complete functional maturation than the hiN cells where the reprogramming genes are constitutively active also in mature neurons.

To circumvent potential positional mutagenesis caused by integrating vectors, we next explored the possibility of converting fibroblast to neurons with nonintegrative vectors. We employed an integration deficient lentiviral vector system that contains a point mutation D64V in the catalytic domain of HIV-1 integrase (Lombardo et al., 2011). When we investigated the expression from our integrative and nonintegrative vectors in HEK293T cells, we could confirm that the nonintegrating vectors were rapidly diluted upon cell proliferation (Figure S3A), which is in line with the nonintegrative nature of the vector. When using these vectors with the same conversion protocol as the integrating vectors, we did observe hiN cell conversion but at a low efficiency (Figures S3B and S3C). However, this could be overcome by minimizing proliferation after transduction by altering the culture conditions so that cells were switched to neuronal medium before transduction (Figure 3A) and either increasing the vector load or the number of vector transductions. In this way, we reached conversion efficiencies of close to 15% (Figure 3B). In the final step, we made nonintegrating vectors with the miR-regulated conversion factors (ABM-miR-124.T-NI versus ABM-miR-124.T). By using a protocol with minimized proliferation after transduction, two transduction events, and high vector concentration, we found that the regulated, nonintegrative vectors converted the fibroblasts at similar efficiency, purity, and morphology as their nonregulated counterparts (Figures 3C–3F). No iN cells were detected in untransduced control cells cultured and analyzed in parallel. When comparing the nonintegrative (NI) vector-based conversions, the ABM-miR-124.T was superior to the nonregulated ABM group in the ability to evoke action potentials (Figures 3G–3I) as well as inward sodium current (Figures 3J and 3K). All of the recorded ABM-miR-124.T-NI-regulated hiN (n = 7) showed single action potential (AP) after current injections as well as inward sodium current (Figures 3G, 3I, and 3K), and one cell showed postsynaptic currents (Figure 3L). For the NI ABM nonregulated group, only one neuron fired action potentials at current injection, whereas all the others showed no AP and no inward sodium current (Figures 3G, 3H, and 3J, n = 5).

DISCUSSION

A growing number of studies report successful direct neural conversion from various somatic cells and from stem cells to functional neurons (Caiazzo et al., 2011; Karow et al., 2012; Pang et al., 2011; Pfisterer et al., 2011a; Son et al., 2011; Vierbuchen et al., 2010; Zhang et al., 2013) and also direct conversion of somatic cells into a variety of mature, clinically relevant cell types such as oligodendrocytes, cardiomyocytes, and hepatocytes (Ieda et al., 2010; Sekiya and Suzuki, 2011; Yang et al., 2013). Because direct conversion does not involve a stem cell intermediate, it has some clear benefits when it comes to developing the cells for clinical use. However, today's techniques for direct conversion typically use integrating vectors that carry a risk of genomic modifications and positional mutagenesis with the insertion of transgenes (Lombardo et al., 2011; Nienhuis et al., 2006; Okita et al., 2008). An added complication during direct conversion is that the copy number of the integrated provirus and the random genomic integration invariably will result in cell populations that are highly heterogeneous from a genomic standpoint.

In this study, we demonstrate that hiN cells can be obtained using self-regulating and nonintegrating vectors that are suitable for use in patients. Using this system, we demonstrate highly efficient conversion of human fibroblast into functional neurons. We show that the neurons survive and mature for up to 90 days in culture, and that microRNA-mediated downregulation of the neural conversion genes allows for a more complete functional maturation of the cells in culture. The high efficiency, combined with the self-regulated and nonintegrative features of this system, represents an important step toward clinical translation of human induced neurons (hiNs).

EXPERIMENTAL PROCEDURES

Cell-Culture Procedures

HFL1 (ATCC-CCL-153) cells were obtained from the American Type Culture Collection (www.lgcstandards-atcc.org/products/all/CCL-153). For neuronal conversion, fibroblasts were plated in mouse embryonic fibroblast (MEF) medium at a density of 26,000 cells per cm^2 in tissue culture plates (Nunc) for conversion with integrative or nonintegrative viral vectors and 130,000 cells per cm^2 for nonintegrative viral vectors. To generate induced neurons from integrative vectors, cells were grown for 3 days posttransduction in MEF

Figure 2. miR-124.T-Regulated Factors Generate hiN at Similar Efficiency as Unregulated Factors

(A and B) Quantification of conversion efficiency (A) and purity (B) of conversion factors with or without miR-124.T regulation (n = 3).

(C) qPCR analysis of resulting iN cells.

(D–G) Neuronal marker MAP2 and NeuN (D and E) and MAP2 and synaptophysin (F and G) are expressed in hiN converted with regular conversion factors (D and F) and miR-124.T-regulated conversion factors (E and G).

(H–P) Whole-cell patch-clamp measurement of miR-124.T-regulated hiN compared to nonregulated hiN. (H) Pie chart of the different responses after current induction to evoke action potential (AP). (I and J) Representative IV diagrams of different responses recorded. (K) ABM-miR124.T-regulated hiN showed a higher number of APs after current injections of 30 and 40 pA compared to nonregulated ABM group suggesting a more mature phenotype. (L–M) Inward sodium- and outward potassium-rectifying currents evoked by depolarizing steps to the cell. (N) Regulated ABM-miR-124.T showed greater inward sodium current compared to nonregulated group but similar potassium-outward currents.

(O) Both groups showed spontaneous postsynaptic currents. (P) At 90 days postconversion, the regulated group showed spontaneous firing at their resting membrane potential, suggesting an integration of the hiN to the surrounding synaptic network.

Scale bar, 100 μm. See also Figure S2.

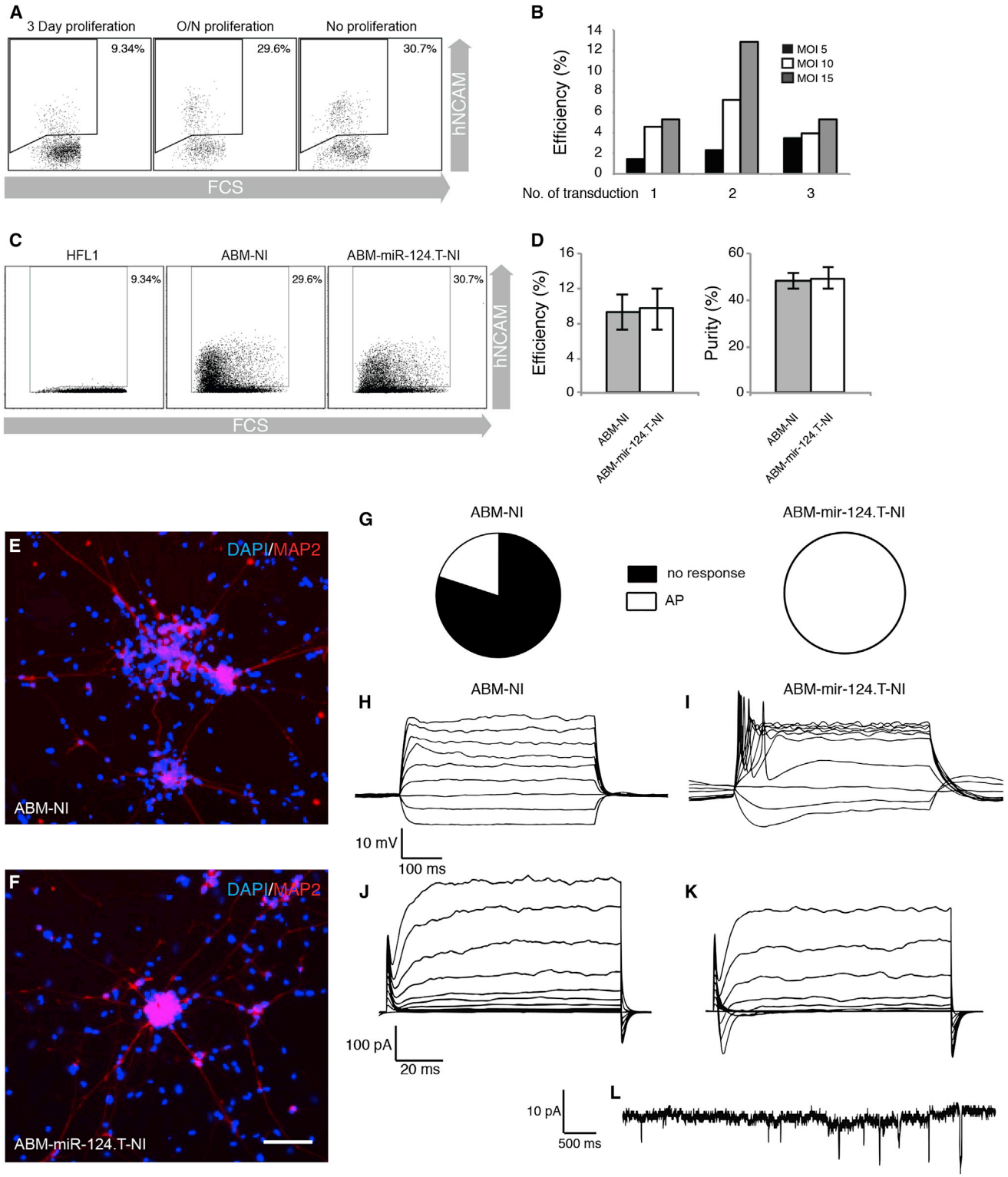

Figure 3. Nonintegrative miR-124.T-Regulated Factors Generate hiN

(A) Proportion of hNCAM-positive cells in ABM nonintegrative (NI) hiN culture increases upon reduction of fibroblast proliferation.

(B) Conversion efficiency of various number of transduction and moi of nonintegrative conversion factors (n = 1).

(C) Flow cytometry analysis of hNCAM-positive cells of day 24 hiN culture.

(D) Quantification of conversion efficiency and purity of nonintegrative conversion factors with or without miR-124.T regulation (n = 3).

(legend continued on next page)

medium before changing to neuronal medium containing Ndiff 227 medium (STEMCELL Technologies), supplemented with neural trophic factors 10 ng ml^{-1} BDNF (R&D Systems) or 2 ng ml^{-1} LM-22A4 (R&D Systems), 2 ng ml^{-1} GDNF, 10 ng ml^{-1} NT3 (R&D Systems), and 0.5 mM db-cAMP (Sigma-Aldrich). Small molecules at the following final concentrations were supplemented on the first 14 days of neuronal medium application: CHIR99021 (2 μM, Axon), SB-431542 (10 μM, R&D Systems), noggin (100 ng ml^{-1}, R&D Systems), and LDN-193189 (0.5 μM, Axon). For neuronal conversion with nonintegrative vectors, fibroblasts were either grown in MEF medium either overnight or for 3 days posttransduction in MEF medium before changing to neuronal medium, or changed to neuronal medium the day after plating, and then the cells were transduced 3 days afterward.

Generation of EGFP-Expressing Cell Line

Lentiviral constructs with PGK-GFP and PGK-GFP-miR-124.T was used to transduce HFL1. See Supplemental Experimental Procedures for details.

Flow Cytometry Analysis and Cell Sorting

For flow cytometry analysis and cell sorting information, see Supplemental Experimental Procedures.

Viral Vectors and Virus Transduction

Six lentiviral vectors expressing mouse open reading frames (ORFs) for *Ascl1*, *Brn2*, and *Myt1l*, with or without miR-124.T regulatory unit sequence, were generated by replacing GFP in a third-generation lentiviral vector containing a nonregulated, ubiquitous phosphorglycerate kinase promoter with the various ORFs (Figure S2A). Third-generation lentiviral vectors were produced as previously described (Zufferey et al., 1997) and titrated by quantitative PCR analysis (Georgievska et al., 2004). Transduction was always performed at moi 5 for integrative vectors and moi 5, 10, 15 as stated for nonintegrative factors. For electrophysiology and quantifications, HFL1 cells were transduced with regulated and unregulated integrative vectors at an moi of 5, and with regulated and unregulated nonintegrative vectors with and moi 10 repeated twice.

Immunocytochemistry

Cells were fixed in 4% paraformaldehyde and preincubated for 15 min in blocking solution (5% normal serum and 0.25% Triton-X in 0.1 M potassium-buffered PBS). The primary antibodies (Table S1) were diluted in the blocking solution and applied overnight at 4°C. Fluorophore-conjugated secondary antibodies (Molecular Probes or Jackson ImmunoResearch Laboratories) were diluted in blocking solution and applied for 2 hr followed by three rinses in potassium PBS.

qRT-PCR Analysis for mir-124 and Subtype-Specific Gene Expression

Total RNA, including miRNA, was extracted from unconverted human fibroblast, sorted hNCAM-positive and -negative cells using the miRNeasy kit (QIAGEN) followed by Universal cDNA synthesis kit (Fermentas, for subtype analysis; Exiqon for miRNA expression). Specifications of these procedures are detailed in Supplemental Experimental Procedures.

Quantifications and Efficiency Calculation

All quantifications were calculated based on data from minimum of three independent experiments. To quantify the conversion efficiency (Vierbuchen et al., 2010), total number of hNCAM-positive cells at the time point of analysis (12 and 24 days as stated) was divided by the number of fibroblasts initially plated for conversion. To determine neuronal purity (Ladewig et al., 2012), the number of hNCAM-positive cells was divided by the total number of cells (as determined by DAPI) present at the time point of quantification (12 and 24 days as stated).

Electrophysiology

For electrophysiology information, see Supplemental Experimental Procedures.

Statistical Analysis

All data are expressed as mean ± SD of the mean. An alpha level of $p < 0.05$ was set for significance. A two-tailed Student's t test was used to compare the downregulation GFP in converted HFL1-GFP and HFL1-GFP-mir-124.T cells, difference in conversion efficiency, purity, and electrophysiological properties between mir-124.T-regulated and -nonregulated ABM-converted cells.

SUPPLEMENTAL INFORMATION

Supplemental Information includes Supplemental Experimental Procedures, three figures, and one table and can be found with this article online at http://dx.doi.org/10.1016/j.celrep.2014.11.017.

AUTHOR CONTRIBUTIONS

S.L. planned, conducted, and analyzed experiments. D.R.O. performed and analyzed electrophysiology experiments, and J.J. and M.P. conceived study and analyzed data. M.P. supervised all parts of study and wrote manuscript. All authors reviewed and gave input to the figures and manuscript.

ACKNOWLEDGMENTS

We thank Ingar Nilsson and Christina Isaksson for technical assistance, Luigi Naldini and Bernhard Gentner for providing lentiviral constructs, and Hakan Toresson for discussions and proofreading of manuscript. The research leading to these results has received funding from the European Research Council under the European Union's Seventh Framework Programme: FP/2007-2013 NeuroStemcellRepair (no. 602278) and ERC Grant Agreement no. 30971, the Swedish Research Council (grant agreement 521-2012-5624 and 70862601/Bagadilico), Swedish Parkinson Foundation (Parkinsonfonden), Leif Jonsons Minnesfond, and the Strategic Research Area at Lund University Multipark (Multidisciplinary research in Parkinson's disease).

Received: July 3, 2014
Revised: October 22, 2014
Accepted: November 10, 2014
Published: December 4, 2014

REFERENCES

Åkerblom, M., Sachdeva, R., Barde, I., Verp, S., Gentner, B., Trono, D., and Jakobsson, J. (2012). MicroRNA-124 is a subventricular zone neuronal fate determinant. J. Neurosci. *32*, 8879–8889.

Åkerblom, M., Sachdeva, R., Quintino, L., Wettergren, E.E., Chapman, K.Z., Manfre, G., Lindvall, O., Lundberg, C., and Jakobsson, J. (2013). Visualization and genetic modification of resident brain microglia using lentiviral vectors regulated by microRNA-9. Nat. Commun. *4*, 1770.

Ambasudhan, R., Talantova, M., Coleman, R., Yuan, X., Zhu, S., Lipton, S.A., and Ding, S. (2011). Direct reprogramming of adult human fibroblasts to functional neurons under defined conditions. Cell Stem Cell *9*, 113–118.

Brown, B.D., Gentner, B., Cantore, A., Colleoni, S., Amendola, M., Zingale, A., Baccarini, A., Lazzari, G., Galli, C., and Naldini, L. (2007). Endogenous

(E and F) Neuronal marker MAP2 is expressed in hiN converted with nonintegrative conversion factors (E) and miR-124.T-regulated conversion factors (F). (G–L) Whole-cell patch-clamp measurement of miR-124.T-regulated nonintegrative (NI) hiN compared to nonregulated NI hiN. (G) Pie chart of the different responses after current induction to evoke action potential (AP) in the two groups and below a representative IV diagram of current injection (H, n = 5 where only one showed AP) (I, n = 7 where all cells showed AP after current injection). (J) None of the recorded cells in the ABM-NI group showed inward sodium current, whereas all of the cells in regulated group did (K). (L) One cell in the ABM-miR124.T. NI group showed postsynaptic currents.
Scale bar, 100 μm. See also Figure S3.

microRNA can be broadly exploited to regulate transgene expression according to tissue, lineage and differentiation state. Nat. Biotechnol. *25*, 1457–1467.

Caiazzo, M., Dell'Anno, M.T., Dvoretskova, E., Lazarevic, D., Taverna, S., Leo, D., Sotnikova, T.D., Menegon, A., Roncaglia, P., Colciago, G., et al. (2011). Direct generation of functional dopaminergic neurons from mouse and human fibroblasts. Nature *476*, 224–227.

Cheng, L.C., Pastrana, E., Tavazoie, M., and Doetsch, F. (2009). miR-124 regulates adult neurogenesis in the subventricular zone stem cell niche. Nat. Neurosci. *12*, 399–408.

Davila, J., Chanda, S., Ang, C.E., Südhof, T.C., and Wernig, M. (2013). Acute reduction in oxygen tension enhances the induction of neurons from human fibroblasts. J. Neurosci. Methods *216*, 104–109.

Dell'Anno, M.T., Caiazzo, M., Leo, D., Dvoretskova, E., Medrihan, L., Colasante, G., Giannelli, S., Theka, I., Russo, G., Mus, L., et al. (2014). Remote control of induced dopaminergic neurons in parkinsonian rats. J. Clin. Invest. *124*, 3215–3229.

Gentner, B., and Naldini, L. (2012). Exploiting microRNA regulation for genetic engineering. Tissue Antigens *80*, 393–403.

Georgievska, B., Jakobsson, J., Persson, E., Ericson, C., Kirik, D., and Lundberg, C. (2004). Regulated delivery of glial cell line-derived neurotrophic factor into rat striatum, using a tetracycline-dependent lentiviral vector. Hum. Gene Ther. *15*, 934–944.

Gossen, M., and Bujard, H. (1992). Tight control of gene expression in mammalian cells by tetracycline-responsive promoters. Proc. Natl. Acad. Sci. USA *89*, 5547–5551.

Ieda, M., Fu, J.D., Delgado-Olguin, P., Vedantham, V., Hayashi, Y., Bruneau, B.G., and Srivastava, D. (2010). Direct reprogramming of fibroblasts into functional cardiomyocytes by defined factors. Cell *142*, 375–386.

Karow, M., Sánchez, R., Schichor, C., Masserdotti, G., Ortega, F., Heinrich, C., Gascón, S., Khan, M.A., Lie, D.C., Dellavalle, A., et al. (2012). Reprogramming of pericyte-derived cells of the adult human brain into induced neuronal cells. Cell Stem Cell *11*, 471–476.

Krichevsky, A.M., Sonntag, K.C., Isacson, O., and Kosik, K.S. (2006). Specific microRNAs modulate embryonic stem cell-derived neurogenesis. Stem Cells *24*, 857–864.

Ladewig, J., Mertens, J., Kesavan, J., Doerr, J., Poppe, D., Glaue, F., Herms, S., Wernet, P., Kögler, G., Müller, F.J., et al. (2012). Small molecules enable highly efficient neuronal conversion of human fibroblasts. Nat. Methods *9*, 575–578.

Liu, M.L., Zang, T., Zou, Y., Chang, J.C., Gibson, J.R., Huber, K.M., and Zhang, C.L. (2013). Small molecules enable neurogenin 2 to efficiently convert human fibroblasts into cholinergic neurons. Nat. Commun. *4*, 2183.

Lombardo, A., Cesana, D., Genovese, P., Di Stefano, B., Provasi, E., Colombo, D.F., Neri, M., Magnani, Z., Cantore, A., Lo Riso, P., et al. (2011). Site-specific integration and tailoring of cassette design for sustainable gene transfer. Nat. Methods *8*, 861–869.

Nienhuis, A.W., Dunbar, C.E., and Sorrentino, B.P. (2006). Genotoxicity of retroviral integration in hematopoietic cells. Mol. Ther. *13*, 1031–1049.

Okita, K., Ichisaka, T., and Yamanaka, S. (2007). Generation of germline-competent induced pluripotent stem cells. Nature *448*, 313–317.

Okita, K., Nakagawa, M., Hyenjong, H., Ichisaka, T., and Yamanaka, S. (2008). Generation of mouse induced pluripotent stem cells without viral vectors. Science *322*, 949–953.

Pang, Z.P., Yang, N., Vierbuchen, T., Ostermeier, A., Fuentes, D.R., Yang, T.Q., Citri, A., Sebastiano, V., Marro, S., Südhof, T.C., and Wernig, M. (2011). Induction of human neuronal cells by defined transcription factors. Nature *476*, 220–223.

Pereira, M., Pfisterer, U., Rylander, D., Torper, O., Lau, S., Lundblad, M., Grealish, S., and Parmar, M. (2014). Highly efficient generation of induced neurons from human fibroblasts that survive transplantation into the adult rat brain. Sci. Rep. *4*, 6330.

Pfisterer, U., Kirkeby, A., Torper, O., Wood, J., Nelander, J., Dufour, A., Björklund, A., Lindvall, O., Jakobsson, J., and Parmar, M. (2011a). Direct conversion of human fibroblasts to dopaminergic neurons. Proc. Natl. Acad. Sci. USA *108*, 10343–10348.

Polo, J.M., Anderssen, E., Walsh, R.M., Schwarz, B.A., Nefzger, C.M., Lim, S.M., Borkent, M., Apostolou, E., Alaei, S., Cloutier, J., et al. (2012). A molecular roadmap of reprogramming somatic cells into iPS cells. Cell *151*, 1617–1632.

Sachdeva, R., Jönsson, M.E., Nelander, J., Kirkeby, A., Guibentif, C., Gentner, B., Naldini, L., Björklund, A., Parmar, M., and Jakobsson, J. (2010). Tracking differentiating neural progenitors in pluripotent cultures using microRNA-regulated lentiviral vectors. Proc. Natl. Acad. Sci. USA *107*, 11602–11607.

Sekiya, S., and Suzuki, A. (2011). Direct conversion of mouse fibroblasts to hepatocyte-like cells by defined factors. Nature *475*, 390–393.

Son, E.Y., Ichida, J.K., Wainger, B.J., Toma, J.S., Rafuse, V.F., Woolf, C.J., and Eggan, K. (2011). Conversion of mouse and human fibroblasts into functional spinal motor neurons. Cell Stem Cell *9*, 205–218.

Takahashi, K., and Yamanaka, S. (2006). Induction of pluripotent stem cells from mouse embryonic and adult fibroblast cultures by defined factors. Cell *126*, 663–676.

Vierbuchen, T., Ostermeier, A., Pang, Z.P., Kokubu, Y., Südhof, T.C., and Wernig, M. (2010). Direct conversion of fibroblasts to functional neurons by defined factors. Nature *463*, 1035–1041.

Wang, P., Zhang, H.L., Li, W., Sha, H., Xu, C., Yao, L., Tang, Q., Tang, H., Chen, L., and Zhu, J. (2014). Generation of patient-specific induced neuronal cells using a direct reprogramming strategy. Stem Cells Dev. *23*, 16–23.

Wapinski, O.L., Vierbuchen, T., Qu, K., Lee, Q.Y., Chanda, S., Fuentes, D.R., Giresi, P.G., Ng, Y.H., Marro, S., Neff, N.F., et al. (2013). Hierarchical mechanisms for direct reprogramming of fibroblasts to neurons. Cell *155*, 621–635.

Yang, N., Zuchero, J.B., Ahlenius, H., Marro, S., Ng, Y.H., Vierbuchen, T., Hawkins, J.S., Geissler, R., Barres, B.A., and Wernig, M. (2013). Generation of oligodendroglial cells by direct lineage conversion. Nat. Biotechnol. *31*, 434–439.

Yoo, A.S., Sun, A.X., Li, L., Shcheglovitov, A., Portmann, T., Li, Y., Lee-Messer, C., Dolmetsch, R.E., Tsien, R.W., and Crabtree, G.R. (2011). MicroRNA-mediated conversion of human fibroblasts to neurons. Nature *476*, 228–231.

Zhang, Y., Pak, C., Han, Y., Ahlenius, H., Zhang, Z., Chanda, S., Marro, S., Patzke, C., Acuna, C., Covy, J., et al. (2013). Rapid single-step induction of functional neurons from human pluripotent stem cells. Neuron *78*, 785–798.

Zufferey, R., Nagy, D., Mandel, R.J., Naldini, L., and Trono, D. (1997). Multiply attenuated lentiviral vector achieves efficient gene delivery in vivo. Nat. Biotechnol. *15*, 871–875.

Cell Reports, Volume *9*

Supplemental Information

Direct Neural Conversion from Human Fibroblasts Using Self-Regulating and Nonintegrating Viral Vectors

Shong Lau, Daniella Rylander Ottosson, Johan Jakobsson, and Malin Parmar

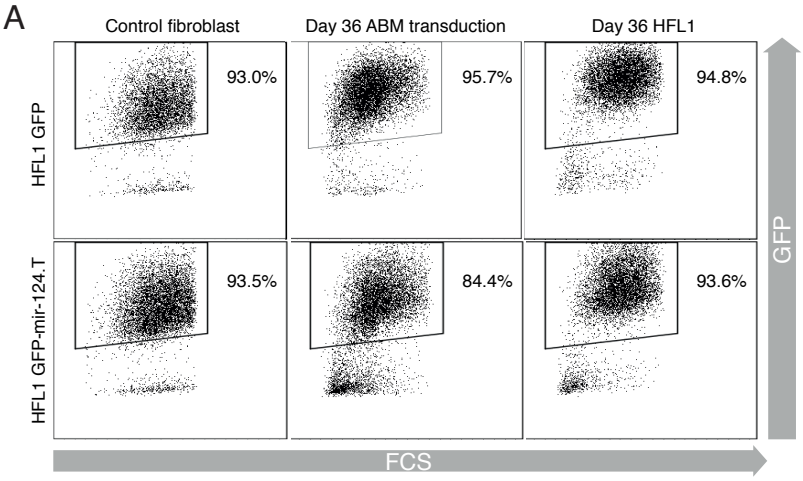
A
Control fibroblast
Day 36 ABM transduction
Day 36 HFL1
HFL1 GFP
HFL1 GFP-mir-124.T
93.0%
95.7%
94.8%
93.5%
84.4%
93.6%
GFP
FCS

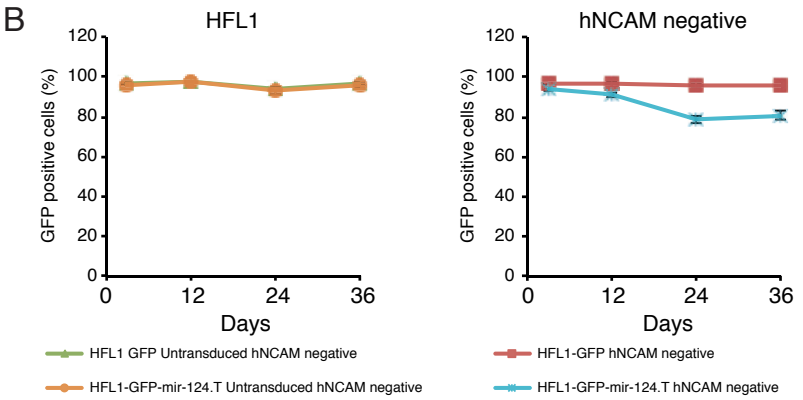
B
HFL1
hNCAM negative
GFP positive cells (%)
Days
HFL1 GFP Untransduced hNCAM negative
HFL1-GFP-mir-124.T Untransduced hNCAM negative
HFL1-GFP hNCAM negative
HFL1-GFP-mir-124.T hNCAM negative

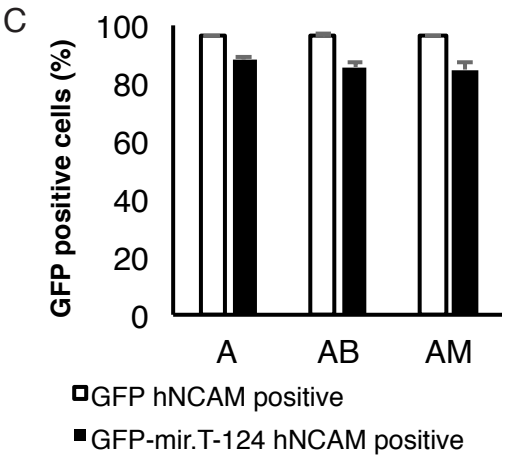
C
GFP positive cells (%)
A
AB
AM
GFP hNCAM positive
GFP-mir.T-124 hNCAM positive

Figure S1 (related to Figure 1).

(A) Flow cytometry analysis of GFP positivity in hNCAM negative cells of day 36 hiN culture. (B) Quantification of GFP positive cell in untransduced and hNCAM negative cells of hiN culture at various maturation stage (n=3). (C) Quantification of GFP positive cell in hNCAM positive population of day 36 hiN converted with Ascl1 only or in combination with Brn2 and Myt1L (n=3).

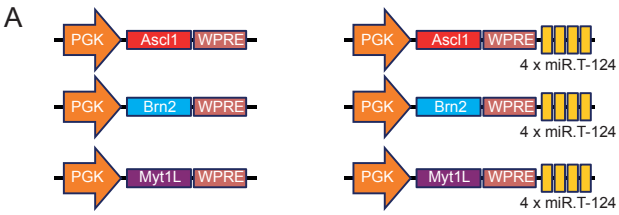
A
PGK
Ascl1
WPRE
PGK
Brn2
WPRE
PGK
Myt1L
WPRE
PGK
Ascl1
WPRE
4 x miR.T-124
PGK
Brn2
WPRE
4 x miR.T-124
PGK
Myt1L
WPRE
4 x miR.T-124

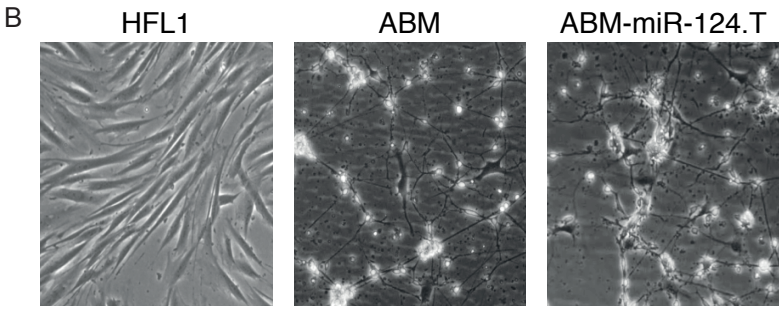
B
HFL1
ABM
ABM-miR-124.T

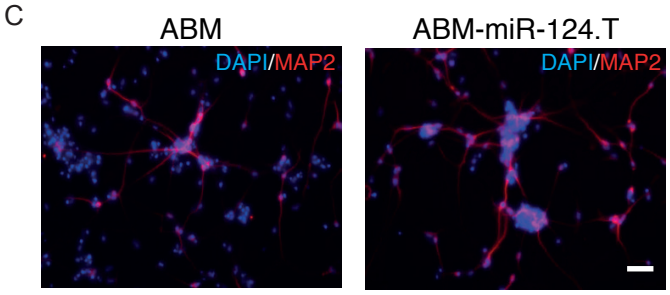
C
ABM
DAPI/MAP2
ABM-miR-124.T
DAPI/MAP2

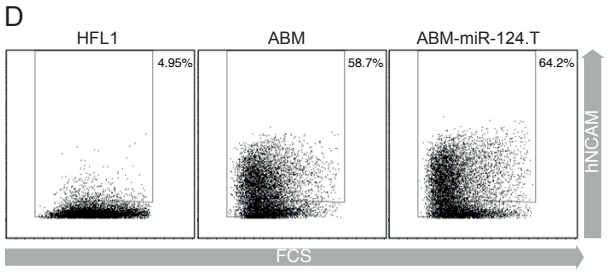
D
HFL1
ABM
ABM-miR-124.T
4.95%
58.7%
64.2%
hNCAM
FCS

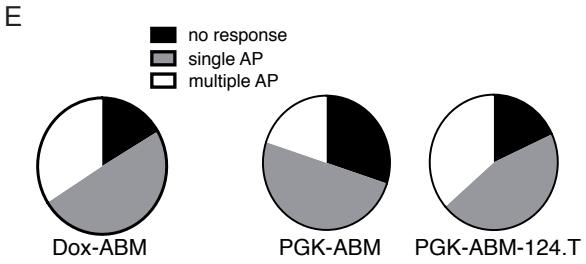
E
no response
single AP
multiple AP
Dox-ABM
PGK-ABM
PGK-ABM-124.T

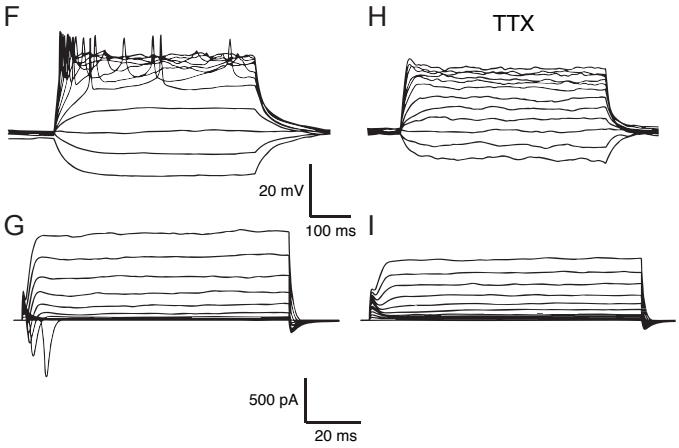
F
20 mV
100 ms
H
TTX
G
I
500 pA
20 ms

Figure S2 (related to Figure 2).

(A) Vector design schematics of regulated (right panel) and non-regulated (left panel) conversion factors. (B) Morphology change was observed in both regular and miR-124.T regulated factors generate hiN on day 12 post transduction. (C) MAP2 expressing hiN is detected in Day 24 conversion culture with both regular and miR-124.T regulated factors. (D) Flow cytometry analysis of hNCAM positive cells in day 24 hiN culture (E) Responses of AP in hiN converted with either Doxycycline regulated promotors (DOX-ABM, n=2 no response, 6 single AP, 4 multiple AP) or the constitutive PGK promotor (PGK-ABM, n=6 no response, 10 single AP, 4 multiple AP and PGK-ABM-miR-124.T, n=2 no response, 5 single AP, 4 multiple AP). (F-I) Both AP (F) and sodium inward current (G) could be blocked with TTX (H,I). Traces represent hiN converted with regulated vectors (PGK-ABM-miR-124.T) but was reproduced also for neurons converted with non regulated vectors (PGK-ABM). Scale bar: 100μm.

A

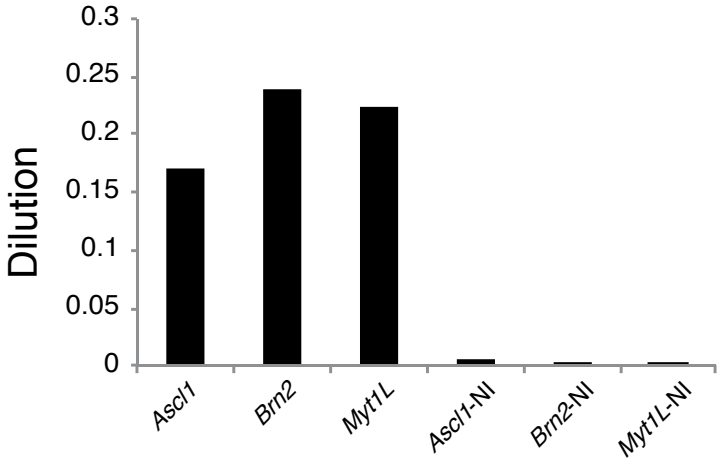
0.3
0.25
0.2
0.15
0.1
0.05
0
Dilution
Ascl1
Brn2
Myt1L
Ascl1-NI
Brn2-NI
Myt1L-NI

B

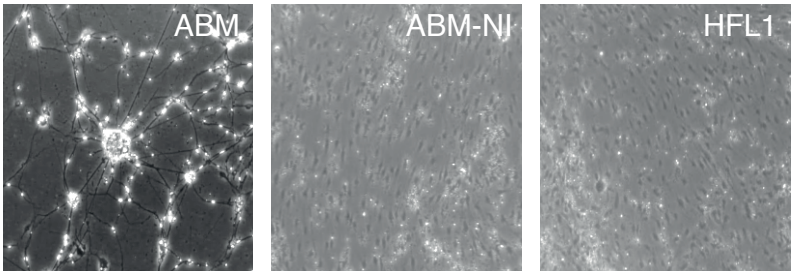
ABM
ABM-NI
HFL1

C

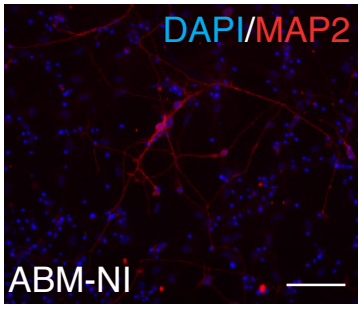
DAPI/MAP2
ABM-NI

Figure S3 (related to Figure 3).

(A) Relative copy number of transgene in HEK293T cells at day ten post transduction of integrative or non-integrative vectors comparing to day one. (B) Representative pictures of morphology in conversion culture with either integrative or non-integrative conversion factors. (C) MAP2 positive cells detected in ABM-NI conversion culture at a low density (Scale bars: 100 μm).

Antibody	Host species	Dilution	Company
MAP2	Mouse	1:250	Sigma
MAP2	Rabbit	1:250	Millipore
hNCAM	mouse	1:200	SantaCruz
hNCAM (CD56)	mouse	1:50	BD Biosciences
NeuN	Mouse	1:200	Millipore
Synaptophysin	Mouse	1:1000	Chemicon

Table S1. List of primary antibody (related to Experimental Procedure, Immunocytochemistry)

Supplemental experimental procedures (related to experimental procedures)

Generation of EGFP expressing cell line: Lentiviral vectors containing a non-regulated, ubiquitous phosphorglycerate kinase promoter expressing EGFP and its miR-124 regulated version which has four miR-124.T sequence cloned downstream of woodchuck hepatitis virus posttranscriptional regulatory element (WPRE) sequence was used to transduce HFL1 cells at a multiplicity of infection (MOI) of 5. The cells were expanded and sorted for GFP positive population with FACSAria III cell sorter (BD Biosciences). Gating was set according to wild type HFL1 cells with no GFP transgene. Cells were sorted into MEF medium and re-plated for further expansion and freezing.

Flow Cytometry analysis and cell sorting: Converted cells were detached from cultureware with either 0.05% trypsin for HFL1 fibroblast or Accutase (PAA Laboratories) for converted iN cell. The cells were triturated and passed through cell strainer cap (70mm) to obtain a single cell suspension and washed with washing buffer containing Hank's balanced salt solution (GIBCO) with 1% bovine serum albumin. The fibroblasts were directly used for sorting according to GFP expression. The converted iN cells were incubated in washing buffer for 15 minutes and then stained with mouse anti hNCAM antibody labelled with APC (BD Biosciences) for 15 minutes at room temperature. The cells were either sorted with FACSAria III cell sorter or analysed with Accuri C6 flow cytometer (BD Biosciences) according to hNCAM expression gated against unconverted fibroblast.

qRT-PCR analysis for mir-124 and subtype specific gene expression: Total RNA, including miRNA, was extracted from unconverted human fibroblast, sorted hNCAM

positive and negative cells using the miRNeasy kit (Qiagen) followed by Universal cDNA synthesis kit (Fermentas, for subtype analysis; Exiqon for miRNA expression). All primers for subtype specific genes were validated on subdissected human tissue and used in analysis of iN samples before (Pereira et al., 2014). LNA–PCR primer sets, hsa-miR-124 and hsa-miR-103 (normalization miRNA), were purchased from Exiqon. All primers were used together with LightCycler 480 SYBR Green I Master (Roche). Standard procedures of qRT-PCR were used, and data were quantified using the ΔΔCt-method.

Electrophysiology: Patch-clamp electrophysiology was performed on hiN at day 60 and 90 post-conversion. Cultured hiNs, with glia, were grown on coverslips and transferred to a recording chamber and submerged in a continuously flowing Krebs solution gassed with 95% O_2 - 5% CO_2 at 28°C. The composition of the standard solution was (in mM): 119 NaCl, 2.5 KCl, 1.3 $MgSO_4$, 2.5 $CaCl_2$, 25 Glucose and 26 $NaHCO_3$. Recordings were made with a Multiclamp 700B amplifier (Molecular Devices), using borosilicate glass pipettes (3–7 MOhm) filled with the following intracellular solution (in mM): 122.5 potassium gluconate, 12.5 KCl, 0.2 EGTA, 10 Hepes, 2 MgATP, 0.3 Na_3GTP and 8 NaCl adjusted to pH 7.3 with KOH as in Pfisterer et al 2011. Data were acquired with pClamp 10.2 (Molecular Devices); current was filtered at 0.1 kHz and digitized at 2kHz.

Cells with neuronal morphology with round cell body were selected for whole-cell patch clamp. Resting membrane potentials were monitored immediately after breaking-in in current-clamp mode. Thereafter, cells were kept at a membrane potential of -60mV to -80mV, and 500ms currents were injected from -20pA to +90pA with 10pA increments to induce action potentials. For sodium and potassium

current measurements cells were clamped at -70mV and voltage-depolarizing steps were delivered for 100ms at 10mV increments. Spontaneous AP were recorded in current-clamp mode at resting membrane potentials.

Vector Dilution assay: Vector dilution assay for the non-integrative constructs was performed with the same method and primer probes as the virus titration with the exception that samples were taken on day1 and day10 post-transduction. Dilution was determined by dividing relative copy number of transgene at day10 by that at day1.